Wuhan University Journal of Natural Sciences Vol. 3 No. 1 1998,35~40

Transmission Electron Microscopy Investigation of the Ar^+ Ion Irradiation Effect in Semiconductor GaAs

Yang Xiangxiu [1,2], **Wang Renhui** [1,2], **Yan Heping**[1], **Zhang Ze**[2]

[1] Department of Physics, Wuhan University, Wuhan 430072, China

[2] Beijing Laboratory of Electron Microscopy, Chinese Academy of Sciences, P.O. Box 2724, Beijing 100080, China

Abstract **Room temperature irradiation effect of GaAs compound semiconductor by 100 keV Ar^+ ions has been systematically studied by means of transmission electron microscopy. The dose dependence of the Ar^+ ion irradiation and room temperature annealing effects have been investigated. The experimental results show that the structure of GaAs transforms from perfect crystalline through weakly and severely damaged crystalline to amorphous states with the increase of the irradiation dose and the damaged states are changed during room temperature annealing.**

Key words **GaAs, irradiation effect, transmission electron microscopy**

Ion implantation is an important and well established technological process in producing microelectronic and optoelectronic devices as well as for the modification of superlattices. An unavoidable drawback of ion irradiation, especially for compound semiconductors, is radiation damage of the substrate, which can lead at high ion implant doses to the formation of a buried or surface amorphous layer. In addition to the researches directed towards ion-beam annealing process[1~4], considerable efforts have been devoted to study the damage in GaAs induced by ion implantation or irradiation over the past few years[5~10].

All the studies have shown that the irradiation effect is dependent on the irradiated materials, the mass and energy of the irradiating ion, its fluence (dose) and dose rate, and also the irradiation temperature. For example the in-situ experiments[8,10] showed that amorphous zones in GaAs created from individual displacement cascades are unstable at temperatures above 250 K. The formation probability and size of the amorphous zones increase with the increase of the ion mass and the decrease of the irradiation temperature from room temperature (RT) to 30 K.

We have irradiated GaAs crystals at RT with 100 keV Ar^+ ions at different doses to introduce some defects or to accelerate the possible phase transitions. The present paper reports the main results on the irradiation effect induced by Ar^+ ion and the subsequent RT annealing effect in GaAs.

1 Experimental details

Te-doped n-type (100)-oriented GaAs single crystals were used in the experiment. Specimens for transmission electron microscopy (TEM) were prepared in the form of 3 mm discs and thinned by mechanical and 4 keV Ar ion-milling without cooling prior to irradiation. The TEM foils were then subjected to irradiation (100 keV Ar^+ ion irradiated at RT) at the same time and stopped (taken out of the machine) one after another when the pre-defined total dose for each foil was reached. Therefore, the foil with higher total dose received initially the same irradiation as the foil with the next lower dose and underwent further irradiation at a higher dose rate. The total dose and the dose rate for

Received Jan. 30,1997. Yang Xiangxiu, born in 1968, Doctor

these foil are listed in Table 1. Subsequent examination of the foils were performed at RT in a Philips CM12 microscope operated at 120 kV. In order to decrease the influence of annealing at RT, all irradiated samples were firstly examined within twelve hours after irradiation. High resolution electron microscopy (HREM) images were taken in a JEOL 2010 microscope operated at 200 kV.

Table 1 Irradiation condition

Total dose /Ar^+ cm^{-2}	Dose rate at additional irradiation/ Ar^+ cm^{-2} s^{-1}
10^{12}	2.5×10^{10}
10^{13}	2.5×10^{11}
10^{14}	5.6×10^{11}
10^{15}	9.5×10^{11}
10^{16}	27.5×10^{11}

The defects produced by ion irradiation were imaged under dynamical two-beam bright-field (BF) and dark-field (DF) conditions with the fundamental reflections (220) and (400) and the superlattice reflection (200). The fundamental reflections are sensitive to lattice strains, e. g., around small dislocation loops, and the difference between the amorphous and crystalline materials whereas the superlattice reflection is additionally sensitive to antisite disorders[8,9].

The projected range which is simulated by running the TRIM91 program is 65. 8 nm with 36. 1 nm longitudinal straggling and 36. 9 nm lateral straggling when the crystalline GaAs is bombarded by 100 keV Ar ions. Hence the damaged depth is comparable with the thin region of the TEM foils.

2 Results

2. 1 Dose dependence of the Ar^+ ion irradiation effect

The Ar^+ ion irradiation effect is strongly dose-dependent as revealed by Fig. 1. When the dose is low ($\leqslant10^{13}$ Ar^+ cm^{-2}), the samples still remain crystalline but weakly damaged. With increasing irradiation dose, crystalline GaAs has a tendency to transform to amorphous state.

The [001] zone axis electron diffraction patterns (EDPs) in Figs. 1(a), (c) and (e) for the virgin specimen and specimens irradiated to doses of 10^{12} and 10^{13} Ar^+ cm^{-2} respectively indicate that GaAs single crystals remain a single crystals when the irradiation dose is equal or less than 10^{13} Ar^+ cm^{-2}. Their (220) two-beam BF and DF images show some small defects surrounded by distinct strain fields. Fig. 1(b) is a (220) DF image of the original GaAs sample which shows black-white lobe (marked by short arrowhead) and black or white dot contrast. According to Ivey *et al.*[11], these small defects were located at the surface of the sample and were introduced by Ar^+ ion milling during preparation of TEM samples. They were identified as two types of defects: One type is small dislocation loops; the other type is local amorphous zones. According to Vetrano *et al.*[8], we measured the size of the defects which is the length of the interface separating the black and white lobes or the maximum dimension of the black dot. In Fig. 1(b) the measured average diameter of the defects is nearly 4 nm.

Figs. 1(d) and (f) are (220) DF micrographs of irradiated samples corresponding to Figs. 1(c) and (e) respectively, which also show black-white lobe (marked by short arrowhead) and black or white dot contrast (coming from both the interior and surface of the foils) just like those in Fig. 1(b) except that the size of the defects increases to approximately 8 nm and the defect density increases with the irradiation dose. It can be seen from Figs. 1(d) and (f) that the direction of no-contrast line separating the black and white lobe is different and is generally not perpendicular to the direction of excited reciprocal vector $\boldsymbol{g}$ under the same two-beam DF condition. This fact indicates that the contrast of black-white lobe comes from small dislocation loops rather than small spherical amorphous regions. In their experiment, Shahid[12] and Wendler[13] also observed similar phenomenon in as-implanted GaAs foils. In addition to those defects described above, another defect is observed by using (200) superlattice reflection. Fig. 2 shows the results. Figs. 2(a), (b) and (c) correspond to Figs. 1(b), (d) and (f) respectively. In Fig. 2 (a), the contrast is homogeneous while in Figs. 2 (b) and (c) there are many black dots contrast with an average diameter of nearly 10 nm which comes from agglomerative antisite defect (disorder)[8]. It can be found that the density of

agglomerative antisite defects and their contrast increase with the increase of the irradiation dose.

Although the samples remain single crystals when the irradiation dose is equal or less than 10^{13} Ar^+ cm^{-2}, it is weakly damaged. Just as described above, there are a lot of small dislocation loops, small amorphous regions and antisite defects (agglomerative or loose) in samples, which lead to some changes in EDPs. For example, the clearness of the Kikuchi lines decreases and the diffuse scattering intensity increases with the increase of the irradiation dose(Figs. 1 a, c, e).

When the dose is high($\geqslant 10^{14}$ Ar^+ cm^{-2}), the GaAs samples have a tendency to transform to amorphous phase as shown in Figs. 1(g) ~ (l) (EDPs and BF images). Figs. 1(g), (i) and (k) (for specimens with doses of 10^{14}, 10^{15} and 10^{16} Ar^+ cm^{-2} respectively) are three very similar EDPs consisting mainly of broad diffraction rings except that there are some weak diffraction spots in Figs. 1(g) and (i). Fig. 1(h)(corresponding to Fig. 1 (g)) is a BF image which shows many small grey dot contrast of about 4 nm in diameter(Ar gas bubbles) distributed in homogeneous background. Additionally, there also exist some large grey contrast (about 40 nm) in Fig. 1(h), which existed in this sample already before 100 keV Ar ions irradiation. Fig. 1(j) (corresponding to Fig. 1(i)) shows the contrast of Ar bubbles with different sizes in homogeneous background, and the maximum size of these gas bubbles is about 15 nm.

Figs. 3(a) and (b) are HREM images of the samples irradiated to doses of 10^{14} and 10^{15} Ar^+ cm^{-2} respectively. It can be clearly seen in Fig. 3 that these specimens were severely damaged, consisting of nanocrystalline grains distributed in amorphous matrix. The size and quantities of the nanocrystalline grains which manifest themselves as lattice fringes decrease with increasing the irradiation dose. For example, many grains of 5 nm in diameter can be seen in Fig. 3(a) while only a few grains of 1 ~ 2 nm are seen in Fig. 3(b). Therefore, we can conclude that the severely damaged GaAs specimens irradiated to doses of 10^{14} and 10^{15} Ar^+ cm^{-2} consist of continuous amorphous phase and some nanocrystalline grains distributed in the amorphous matrix.

Except the contrast of Ar gas bubble with small size (about 2 nm in diameter), Fig. 1(l) (corresponding to Fig. 1(k)) shows uniform, structureless contrast typical of amorphous phase. Combined with Fig. 1(k), this indicates that high dose (10^{16} Ar^+ cm^{-2}) irradiation converts the perfect crystalline GaAs to completely amorphous phase. However, when thick region of the specimen irradiated to the dose of 10^{16} Ar^+ cm^{-2} is observed, both EDP and BF image show a mixture of amorphous and crystalline states.

2.2 Room temperature annealing effect

After put aside at RT for 42 and 80 days, the irradiated samples were systematically observed again. It was found that the main feature of the micrographs and EDPs is similar to that in Fig. 1 with two exceptions. Firstly, Fig. 4(a) shows a (220) DF image from the specimen irradiated to the dose of 10^{13} Ar^+ cm^{-2} and annealed at RT for 42 days where many black-white lobe contrasts from small dislocation loops(marked by short arrowhead) are seen which possess larger size (10 ~ 15 nm) and higher density compared with Fig. 1(f) before annealing. Fig. 4(b) shows a (200) DF image from the same specimen as Fig. 4(a) where many black dots from agglomerative antisite defects are seen which possess smaller size ($\approx$ 5 nm) and higher density compared with Fig. 2(c). Secondly, after 80 days RT annealing only the thin region of the specimens which were amorphized by ion irradiation remains to be completely amorphous. Regions with medium thickness which was amorphized in the as-irradiated foil become mixture of amorphous and crystalline states indicating a partial recrystallization of the amorphous phase during RT annealing.

3 Discussion

In the present work we observed amorphous zones and antisite disorders in the GaAs single crystals irradiated by 100 keV Ar^+ ions to a lower dose ($\leqslant 10^{13}$ Ar^+ cm^{-2}) and complete amorphization in the thin region of the GaAs specimen when the dose is very high (10^{16} Ar^+ cm^{-2}). These observations are in consistence with the existed observations. For example, Vetrano *et al.*[8] observed antisite defects in GaAs sample irradiated by 50 keV Kr^+ ions at 30 K and Wesch *et al*[7] discussed

the formation mechanism of antisite disorder. Bench *et al*[10] observed isolated amorphous zones of 4～8 nm in diameter in GaAs irradiated by 50 keV Ar^+, Kr^+ and Xe^+ ions or 80 keV Au^+ ions at 30 or 300 K to a lower dose (1.9 to 6×10^{11} cm^{-2}). Jencic *et al*[9] observed that crystalline GaAs was completely converted to an amorphous state when irradiated by 1.5 MeV Xe^+ ion to a dose between 10^{14} and 3×10^{14} Xe^+ cm^{-2}(at 300 K) or to a dose of 10^{14} Xe^+ cm^{-2}(at 30 K).

Although most of the studies about irradiation effect of GaAs emphasised only amorphization and sometimes about antisite disorder[8,9,10,14], we have indeed observed black-white lobe contrast in the specimens irradiated to a lower dose ($\leqslant10^{13}$ Ar^+ cm^{-2}) which is typical of the strain contrast produced by small dislocation loops[14,15]. The formation of small dislocation loops may be explained as follows. At the beginning of a displacement cascade induced by an energetic ion Frenkel pairs form. Owing to the faster diffusion of the interstitials compared with vacancies, a vacancy-rich core results in the cascade which favors the formation of a vacancy small dislocation loop.

Since the virgin TEM foils were Ar^+ ion-milled there must exist the same defects as the specimens irradiated by 100 keV Ar^+ ions to a lower dose. Obviously the defect size and density are smaller in the virgin specimen owing to the much lower energy (4 kV) during ion milling. The defect density increases with the increase of the irradiation dose, and lastly the amorphous regions are connected to form a complete amorphous phase.

Because the affecting range of the 100 keV Ar^+ ions is nearly 100 nm, when the upper layer of 100 nm in thickness transformed into amorphous state, the lower layer of the TEM specimen underwent weaker damage and hence remained to be defected crystal. This explains the observed thickness-dependence of the irradiation-induced amorphization behaviour. Why Ar^+ gas bubbles formed during irradiation to the dose of 10^{15} Ar^+ cm^{-2} become much smaller or disappeared during further irradiation to the dose of 10^{16} Ar^+ cm^{-2} may be explained as follows: The formation of gas bubbles behaves like a precipitation of second phase. It needs sufficient concentration of Ar and enough diffusion kinetics, and hence a sufficient high total dose (10^{15} Ar^+ cm^{-2}). However, Ar^+ ion irradiation possesses also a disorder effect which may disrupt gas bubbles and this effect is proportional to the dose rate. Since the irradiation to the dose of 10^{16} Ar^+ cm^{-2} was carried out under a very high dose rate (27.5×10^{11} Ar^+ cm^{-2} s^{-1}), it must disrupt the existed Ar gas bubbles.

While Vetrano *et al*[8] observed a rapid reduction of the amorphous zone density when specimens irradiated with 50 keV Ar^+ ions at 30 K to a dose of 4×10^{11} Ar^+ cm^{-2} were annealed at RT, we observed an increase of the densities of small dislocation loops and antisite defects after RT annealing. Our observation may be explained as follows. In the irradiation-induced antisite defects and small dislocation loops, antisite atoms and vacancies were loosely distributed. After annealing they become more concentrated and hence their size becomes smaller and their contrast becomes stronger so that more defects become discernible. In addition, small dislocation loops with larger size can form through coalescing several smaller dislocation loops adjoining each other by RT annealing.

Moreover, it is reasonable to suppose that the recrystallization process is strongly dependent on the geometry of the amorphous region. An isolated small amorphous zone surrounded by crystals is easier to recrystallize owing to the extensive short-distance diffusion. On the contrary, the recrystallization of a completely amorphous region must begin by nucleation of crystallites in the interior of the amorphous region and is more difficult. The recrystallization behaviour of partially overlapped large amorphous zones induced by irradiation of high-energy and high dose ions lies between. Such a mechanism can explain the observed recrystallization behaviour described in section 2.2 of the paper and the conflicted experimental results in the literature that, on the one hand, Vetrano[8] observed a rapid reduction of the amorphous zone density when specimens irradiated with 50 keV Ar^+ ions at 30 K to a dose of 4×10^{11} Ar^+ cm^{-2} were annealed at RT, while on the other hand, Jencic[9] reported that no recrystallization took place in the GaAs specimens, which were irradiated by 1.5 MeV Xe^+ ions at 30 K to a dose of 10^{14} Xe^+ cm^{-2} and completely amorphized, after warming them to RT.

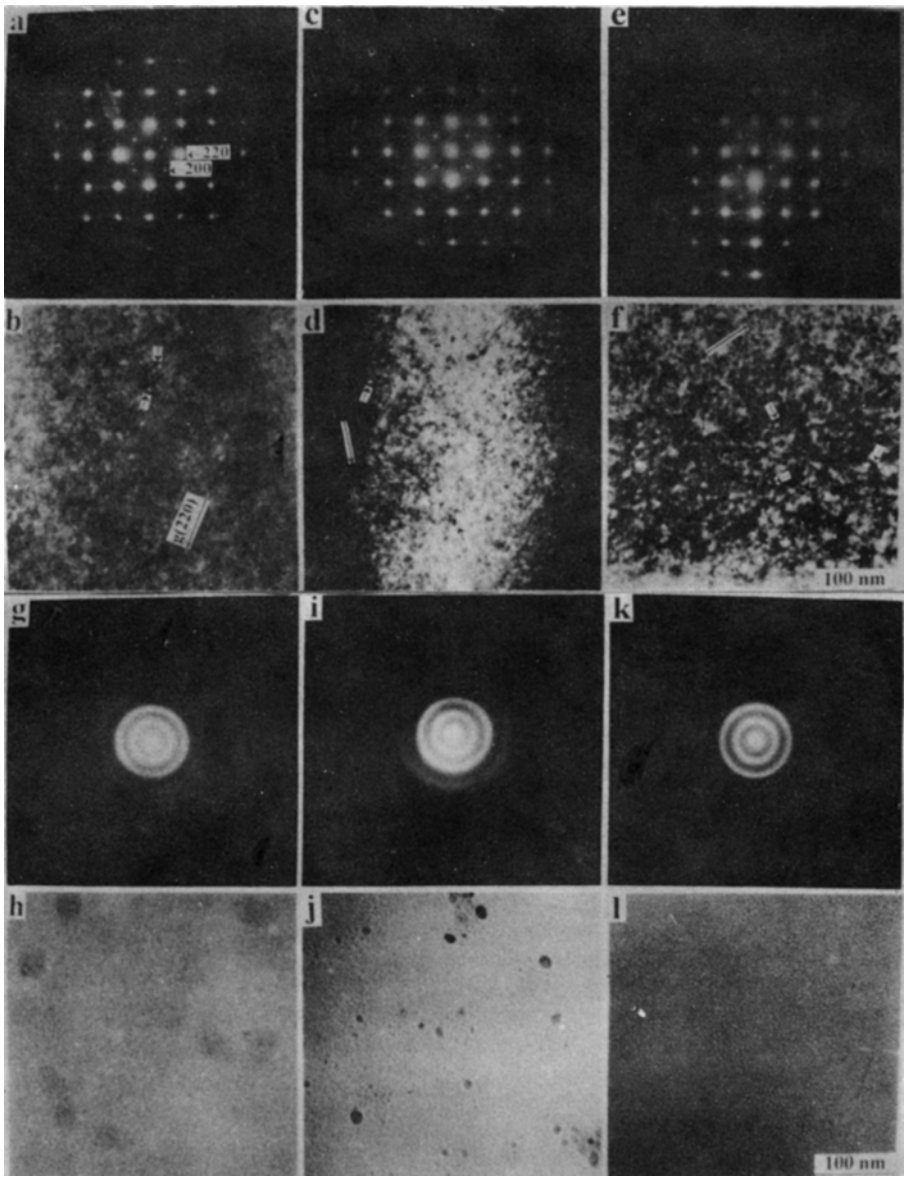

Fig. 1 (a), (c), (e), (g), (i), (k) EDPs, (b), (d), (f) (220) DF images and (h), (j), (l) BF images of GaAs foils. (a), (b) before and (c)~(l) after 100 keV Ar^+ ion irradiation at RT. (c), (d) to a dose of 10^{12} Ar^+ cm^{-2}, (e), (f) to a dose of 10^{13} Ar^+ cm^{-2}, (g), (h) to a dose of 10^{14} Ar^+ cm^{-2}, (i), (j) to a dose of 10^{15} Ar^+ cm^{-2}, (k), (l) to a dose of 10^{16} Ar^+ cm^{-2}. Short arrowheads indicate black-white lobe contrasts and long arrowheads indicate the directions of the excited reciprocal vector $g(220)$

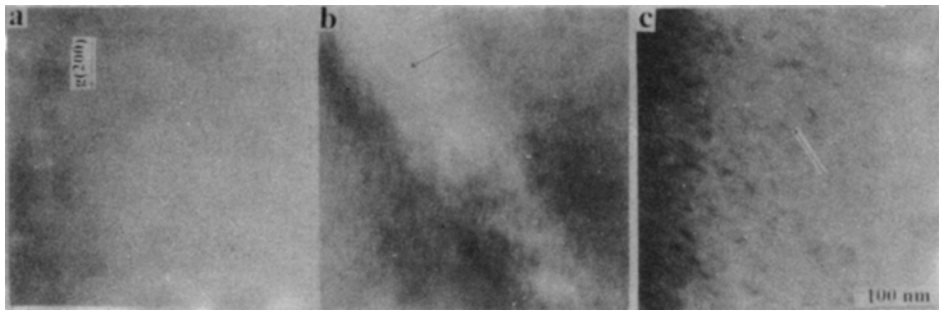

Fig. 2 (200) DF images of the GaAs foils. Before (a) and after 100 keV Ar^+ ion irradiation at RT to doses of 10^{12} Ar^+ cm^{-2} (b) and 10^{13} Ar^+ cm^{-2}(c). Long arrowheads indicate the directions of the excited reciprocal vector $g(200)$

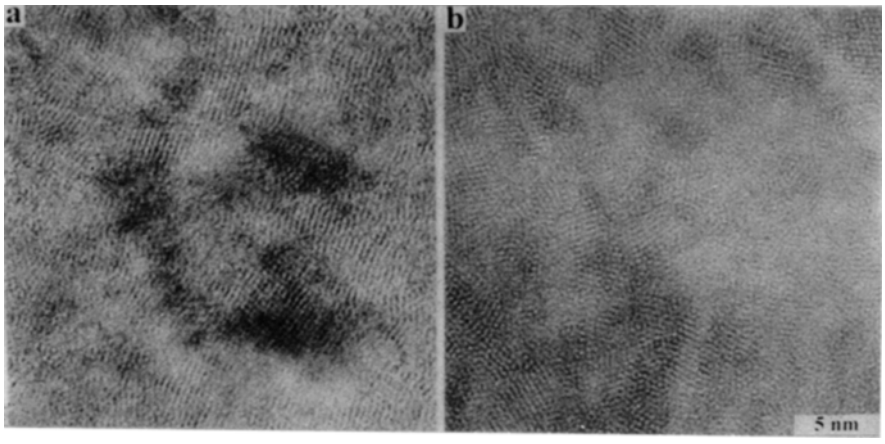

Fig. 3 HREM images of samples irradiated to doses of 10^{14} Ar^+ cm^{-2}(a) and 10^{15} Ar^+ cm^{-2}(b), respectively

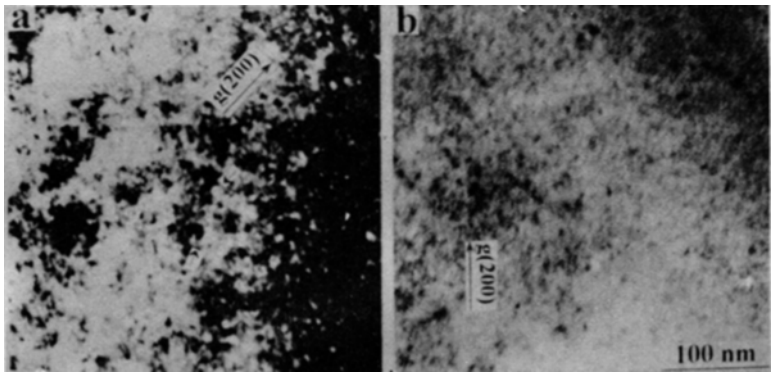

Fig. 4 (a) (220) DF image and (b) (200) DF image of the GaAs foil irradiated to a dose of 10^{13} Ar^+ cm^{-2} and then annealed at RT for 42 days. Short arrowheads indicate black-white lobe contrast

References

1 Sadana D K, Sands T, Washburn J. High resolution transmission electron microscopy study of Se^+-implanted and annealed GaAs: Mechanisms of amorphization and recrystallization. *Appl Phys Lett*, 1984, **44**: 623

2 Wang K W, Spitzer W G, Hubler G K, *et al*. Ion implantation of Si by ^{12}C, ^{29}Si, and ^{120}Sn: Amorphization and annealing effect. *J Appl Phys*, 1985, **58**: 4553

3 Schork R, Pichler P, Kluge A, *et al*. Radiation-enhanced diffusion during high-temperature ion implantation. *Nucl Instr and Meth*, 1991, B**59/60**: 499

4 Alberts H W, Gaigher H L, Bredell L J. Channeling and TEM investigations of pulse electron beam annealed GaAs implanted with Pb. *Nucl Instr and Meth*, 1993, B**80/81**: 519

5 Sadana D K. Mechanisms of amorphization and recrystallization in ion implanted III-V compound semiconductors. *Nucl Instr and Meth*, 1985, B**7/8**: 375

6 Kudo K, Makita Y, Oyanagi H, *et al*. Local structure of heavily Zn^+-implanted GaAs studied by photoluminescence and fluorescence EXAFS. *Nucl Instr and Meth*, 1987, B**19/20**: 398

7 Wesch W, Wendler E, Gotz G, *et al*. Defect production during ion implantation of various $A_{\text{I}}B_{\text{V}}$ semiconductors. *J Appl Phys*, 1989, **65**: 519

8 Vetrano J S, Bench M W, Robertson I M, *et al*. In-situ studies of ion irradiation effects in an electron microscope. *Metallurg Trans*, 1989, A**20**: 2673

9 Jencic I, Bench M W, Robertson I M, *et al*. Comparison of the amorphization induced in $Al_xGa_{1-x}As$ and GaAs by heavy-ion irradiation. *J Appl Phys*, 1991, **69**: 1287

10 Bench M W, Robertson I M, Kirk M A. Transmission electron microscopy investigation of the damage produced in individual displacement cascades in GaAs and GaP. *Nucl Instr and Meth*, 1991, B**59/60**: 372

11 Ivey D G, Piercy G R. Electron microscopy specimens prepared by ion milling. *Thin Solid Films*, 1987, **149**: 73

12 Shahid M A, Sealy B J. The residual microstructure of ion-implanted semi-insulating GaAs. *Radiation Effects*, 1986, **97**: 147

13 Wendler E, Wesch W, Gotz G. Defects in weakly damaged ion-implanted GaAs and other III-V semiconductors. *Phys Stat Sol(a)*, 1989, **112**: 289

14 Bench M W, Tappin D K, Robertson I M. On the suitability of the down-zone imaging technique to the study of radiation damage. *Phil Mag Lett*, 1992, **66**: 39

15 Edington J W. *Practical Electron Microscopy in Materials Science*, Vol. **3**, London: McMillan Press, 1975